

Trends in PET Imaging*

William W. Moses

Lawrence Berkeley National Laboratory, University of California, Berkeley, CA 94720 USA

Abstract

Positron Emission Tomography (PET) imaging is a well established method for obtaining information on the status of certain organs within the human body or in animals. This paper presents an overview of recent trends PET instrumentation. Significant effort is being expended to develop new PET detector modules, especially those capable of measuring depth of interaction. This is aided by recent advances in scintillator and pixellated photodetector technology. The other significant area of effort is development of special purpose PET cameras (such as for imaging breast cancer or small animals) or cameras that have the ability to image in more than one modality (such as PET / SPECT or PET / X-Ray CT).

I. INTRODUCTION

Positron Emission Tomography (PET) is a nuclear medical imaging technique whereby a biologically active compound (*i.e.* a drug) labeled with a positron emitting isotope (usually ^{18}F , ^{11}C , ^{13}N , or ^{15}O) is introduced into the body (in trace quantities) either by injection or inhalation. This compound then accumulates in the patient and the pattern of its subsequent radioactive emissions is used to estimate the distribution of the radioisotope and hence of the tracer compound [1-7].

Since the image that is produced is of the distribution of a drug within the body, PET is capable of targeting where certain metabolic processes occur and measuring the rate at which these processes take place. Thus, it is able to determine whether the biochemical function of an organ is impaired, while many other forms of medical imaging (such as x-ray, ultrasound, or magnetic resonance techniques) are usually confined to determining the physical structure of the organ. It is therefore most frequently used in organs and diseases where biological function is of primary importance and information on physical structure is either irrelevant or ambiguous. Examples are neurological diseases (such as Alzheimer's disease) where physical affects are only observable on a microscopic level, heart disease (where the relative vigor of the tissue is of primary importance), or oncology (cancer), where the metabolic rate gives valuable information on whether tissue is cancerous and how it responds to treatment.

A typical PET camera consists of a planar ring of small photon detectors, with each photon detector placed in time coincidence with *each* of the individual photon detectors on the other side of the ring (Figure 1). When a pair of photon detectors simultaneously detect 511 keV photons, a positron is known to have annihilated somewhere on the line connecting the two detectors. The set of all lines connecting detectors (known as chords) makes the requisite set of

projections to perform computed tomography for a single plane. Multiple detector rings are stacked on top of each other to obtain images from multiple slices, and thus a three-dimensional image of the patient. Planes of tungsten septa placed between detector planes are often used to shield the detectors from Compton scattered photons emanating from other parts of the body, and images taken in this geometry are often known as "2-D PET" images. Coincidences between nearly adjacent "cross-plane" rings are usually added to the closest "direct plane" to increase detection efficiency. If the septa are removed, the efficiency is greatly increased (as coincidences from widely separated planes can be accepted), but the backgrounds also increase significantly. However, the signal to noise ratio improves in some situations, and this mode of operation is known as "3-D PET."

II. PET DETECTOR MODULE TRENDS

The most commonly used PET detector module is known as a block detector, a schematic of which is shown in Figure 2 [8]. A block of BGO scintillator crystal is partially sawn through to make a group of quasi-independent crystals that are optically coupled to four photomultiplier tubes. When a gamma ray interacts in the crystal, the resulting scintillation photons are emitted isotropically but the saw cuts limit (but do not entirely prevent) their lateral dispersion as they travel toward the photomultiplier tubes. The position (*i.e.* crystal element) of the gamma ray interaction is then determined by the analog ratio of the photomultiplier tube output signals, and the gamma ray energy is determined and a timing pulse generated by the sum of these four signals. A typical PET detector module has 80% detection efficiency, 20% fwhm energy resolution, 2 ns fwhm timing resolution, 4 μs dead time, and 5 mm fwhm position resolution for 511 keV gammas [9].

The detector module performance is limited by the BGO scintillator crystal. A scintillator with a faster decay time would improve timing resolution and decrease dead time, while one with a higher light output would improve energy resolution and spatial resolution (by allowing more crystals

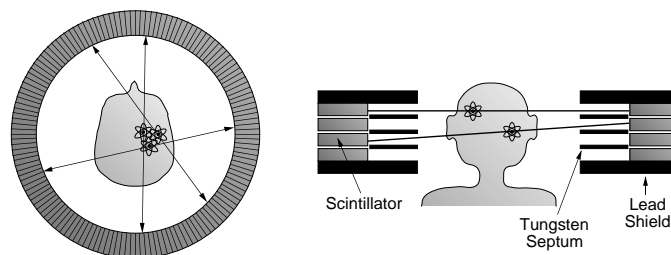


Figure 1. **PET Camera.** The diagram at the left shows a single plane of a PET camera, consisting of a ring of gamma detectors placed around the object to be imaged. When a crystals in opposing hemispheres simultaneously detect 511 keV gammas, a positron is assumed to have annihilated on the line connecting them. Multiple planes are stacked up, as shown on the right to form a volumetric image. Tungsten septa reduce out-of-plane contributions.

* This work was supported in part by the U.S. Department of Energy under Contract No. DE-AC03-76SF00098, and in part by Public Health Service Grants No. R01-CA67911 and P01-HL25840 from the National Institutes of Health.

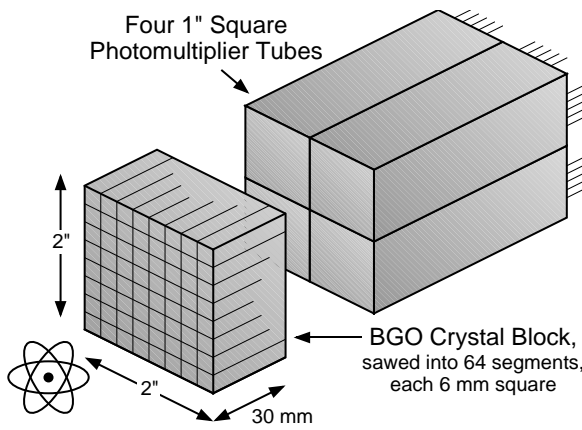


Figure 2. **Conventional PET Detector Module.** Scintillation light from gamma ray interactions is detected by multiple photomultiplier tubes. The interaction position is determined by the ratio of the analog signals, and the energy by the analog sum of the signals.

per block to be unambiguously decoded). However, short attenuation length is critical in order to maintain high spatial resolution (the details are described in the following paragraph), and for this reason BGO dominates. However, some recently developed scintillators are being incorporated in experimental PET systems. Cerium activated lutetium orthosilicate ($\text{Lu}_2\text{SiO}_5\text{:Ce}$ or LSO) exhibits 4 times higher light output and 8 times faster decay time than BGO, while maintaining a similar attenuation length [10]. Although it has self-induced background events from naturally occurring ^{176}Lu , its use for PET is compelling and there is hope that the cost can be reduced enough to make it viable. LSO has been used for a large number of prototype PET detector module designs and a high resolution research PET camera has been made with LSO [11]. Gadolinium orthosilicate ($\text{Gd}_2\text{SiO}_5\text{:Ce}$ or GSO) has 50% higher light output than BGO and 5 times faster decay time, but its attenuation length is 40% longer [12]. This, in addition to a cleavage plane that makes fabrication difficult make GSO a less compelling alternative than LSO, but a brain PET camera using GSO is under construction [13].

In order to increase efficiency and reduce the number of detector modules (and hence cost), PET camera designers would like to reduce the diameter of the detector ring. Unfortunately, they are prevented from doing this by a resolution degradation artifact caused by penetration of the 511 keV photons into the crystal ring. The origin of this artifact, variously known as radial elongation, parallax error, or radial astigmatism, is shown in Figure 3. Photons that impinge on the detector ring at an oblique angle can penetrate into adjacent crystals before they interact and are detected, which causes mis-positioning errors (*i.e.* events are assigned to chords that do not pass through the source). This spatial resolution degradation increases for objects placed further away from the center of the tomograph ring. This artifact can be reduced significantly or eliminated if the detector module is capable of measuring not only the identity of the crystal of interaction but the depth of interaction within that crystal. With such information, the event can be assigned to the chord that connects the interaction points (rather than the interaction crystals), and as that chord will pass through the source, no mispositioning errors are generated.

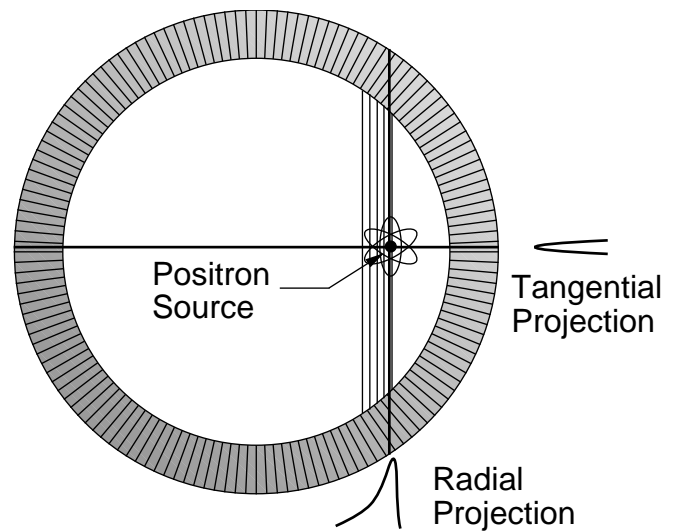


Figure 3. **Cause of Radial Elongation.** 511 keV photons that are incident at an oblique angle can penetrate into the detector ring before interacting and being detected. This causes a blurring that worsens as the source is moved away from the center of the ring.

Developing a detector module capable of accurately measuring this interaction depth is an active field of research. Figure 4 schematically shows three general approaches that have been taken to measure interaction depth. The first, shown in Figure 4a, is a phoswich approach, in which the scintillator block of a conventional PET detector is effectively replaced with two or more layers of different scintillator materials, so each scintillator “pixel” now contains stratified layers of scintillator material [14]. As the different materials possess different scintillation decay times, the readout electronics is modified to perform a crude measurement of the decay time, and so the type of the scintillator that the interaction occurred in (and therefore the interaction depth) is identified. A high resolution research PET camera that utilizes a 15 mm deep phoswich detector made of 7.5 mm deep LSO and GSO crystals has recently been built [15].

The second general technique for measuring depth of interaction shown in Figure 4b is to utilize light sharing. With this approach, each scintillator element is attached to two photodetectors, usually on opposing ends of the crystal. The amount of light observed by each photodetector depends on the interaction position, so the ratio of the two photodetector signals is used to estimate the interaction depth. Recent

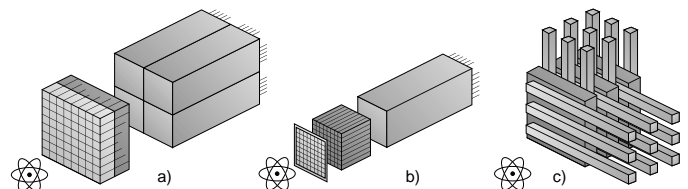


Figure 4. **Depth of Interaction Measurement Concepts.** In a), the scintillator in a conventional PET detector module is stratified in depth with two different scintillator materials – the depth is distinguished by decay time. In b), scintillation light is shared between two photodetectors – the ratio determines the depth. The detector in c) is comprised of a stack of imaging planes – the depth is determined by which layer the interaction is observed in.

advances in pixellated photodetectors have contributed greatly to this design approach. Many combinations of photodetectors have been used, including single anode photomultiplier tubes, PIN photodiode arrays, avalanche photodiode arrays, and multianode photomultiplier tubes [16-19]. At present, no cameras have been built utilizing any of these schemes, although several are under construction.

The third approach for measuring interaction depth, shown in Figure 4c, is to stack multiple layers of two-dimensional detector planes. The plane that the interaction is observed in identifies the depth while 2-D detector provides the other two coordinates. One proposed 2-D detector consists of orthogonal arrays of wavelength-shifting fibers coupled to thin plates of LSO scintillator crystal [20, 21]. The fiber absorbs this primary scintillation light and re-emits lower energy photons, some of which are transported down the length of the fiber and are observed by a position-sensitive photodetector. Another 2-D detector that has been incorporated into a PET camera consists of many thin sheets of lead interspersed with wire chambers [22, 23]. 511 keV interactions in the lead result in some recoil electrons entering the active area of the wire chamber, where they are detected. Such detectors have excellent spatial resolution, but sacrifice both detection efficiency and energy resolution.

III. TRENDS IN PET CAMERA DESIGN

The biggest current trends in PET camera design are specific purpose cameras and cameras that are capable of imaging with two modalities. Conventional whole-body PET cameras can image any part of the body. Their development is mature enough that the main gains to be made are in the cost / performance tradeoff, where only relatively small gains are possible. However, cameras can be optimized for imaging a single organ, which could result in large performance gains at the expense of limited body coverage. A prime example of this is PET cameras optimized for imaging breast cancer, for which there are a number of designs [24-27]. Another field that is growing rapidly is PET cameras for imaging small animals, especially mice and rats. PET's ability to measure biochemical function, rather than structure, can provide crucial insight into the functioning of new and existing pharmaceuticals, the nature of diseases, or the function of specific genes. These experiments are usually performed in small animals, requiring resolutions much higher than those achieved in human PET scanners. By using small scintillator crystals and multianode photomultiplier tubes, spatial resolutions below 2 mm fwhm have been achieved [28-32].

It is often desirable to perform different types of imaging procedures on a single patient. For example, X-ray CT provides excellent anatomical detail while PET provides biochemical information — obtaining both images of the same patient is likely to lead to more accurate diagnosis than either single image would. Thus, devices have recently been built in which an X-ray CT imager and a PET imager have been placed around a single patient bed [33]. While images from both modalities cannot be obtained simultaneously, the ability to perform both studies without repositioning the patient is extremely helpful, especially when imaging the abdomen.

Finally, there has been a strong trend in recent years to equip SPECT cameras (which are optimized to detect 140 keV gamma rays) with coincidence electronics and give them the ability to obtain PET images. The benefits of this are largely economic — SPECT cameras are far more common than dedicated PET cameras and so any hospital with a SPECT camera can, for a relatively small cost, also have the ability to acquire PET images. Some compromises in performance (as compared to dedicated PET cameras) are necessary, but clinically valuable images are often obtained.

IV. CONCLUSION

PET imaging has benefited from recent developments in scintillator materials and pixellated photodetectors, which have enabled a number of detector module designs that are capable of measuring depth of interaction. By measuring depth of interaction, PET camera makers can maintain high spatial resolution with smaller detector ring diameters, simultaneously reducing cost and increasing performance. Recent years have also seen the emergence of special purpose PET cameras, notably for imaging breast cancer or small animals, as well as cameras that also have the ability to obtain SPECT or X-Ray CT images.

V. ACKNOWLEDGMENT

I would like to thank Dr. Stephen Derenzo, Dr. Thomas Budinger, and Dr. Ronald Huesman for many interesting conversations, and would also like to thank Dr. Mats Danielsson for the opportunity to consider the current trends in PET imaging. This work was supported in part by the Director, Office of Science, Office of Biological and Environmental Research, Medical Science Division of the U.S. Department of Energy under Contract No. DE-AC03-76SF00098, and in part by the National Institutes of Health, National Cancer Institute under grant No. R01-CA67911, and National Institutes of Health, National Heart, Lung, and Blood Institute under grant No. P01-HL25840.

VI. REFERENCES

- [1] "Special Issue on Clinical PET," *J. Nucl. Med.*, vol. 32, pp. 561-748, 1991.
- [2] M. P. Sandler, R. E. Coleman, F. J. T. Wackers, et al., *Diagnostic Nuclear Medicine*. Baltimore, MD: Williams & Wilkins, 1996.
- [3] W. R. Hendee and R. Ritenour, *Medical Imaging Physics*. St. Louis, MO: Mosby Year Book, 1992.
- [4] E. Krestel, *Imaging Systems for Medical Diagnosis*. Berlin: Siemens Aktiengesellschaft, 1990.
- [5] A. Macovski, *Medical Imaging Systems*. Englewood Cliffs, NJ: Prentice Hall, 1983.
- [6] S. Webb, *The Physics of Medical Imaging*. Bristol: Institute of Physics Publishing, 1993.
- [7] S. R. Cherry and M. E. Phelps, "Positron Emission Tomography: Methods and Instrumentation," in *Diagnostic Nuclear Medicine*, M. P. Sandler, R. E. Coleman, F. J. T. Wackers, J. A. Patton, A. Gottschalk, and P. B. Hoffer, Eds. Baltimore, MD: Williams & Wilkins, 1996, pp. 139-159.

- [8] S. R. Cherry, M. P. Tornai, C. S. Levin, et al., "A comparison of PET detector modules employing rectangular and round photomultiplier tubes," *IEEE Trans. Nucl. Sci.*, vol. NS-42, pp. 1064–1068, 1995.
- [9] W. W. Moses, S. E. Derenzo, and T. F. Budinger, "PET detector modules based on novel detector technologies," *Nucl. Instr. Meth.*, vol. A-353, pp. 189–194, 1994.
- [10] C. L. Melcher and J. S. Schweitzer, "Cerium-doped lutetium orthosilicate: a fast, efficient new scintillator," *IEEE Trans. Nucl. Sci.*, vol. NS-39, pp. 502–505, 1992.
- [11] M. Schmand, K. Wienhard, M. E. Casey, et al. Performance evaluation of a new LSO high resolution research tomograph-HRRT. Proceedings of The IEEE 1999 Nuclear Science Symposium and Medical Imaging Conference, pp. 1067-1071, vol. 2, paper M04-002, (Edited by J. A. Seibert), Seattle, WA, 1999.
- [12] K. Takagi and T. Fukazawa, "Cerium-activated Gd_2SiO_5 single crystal scintillator," *Appl. Phys. Lett.*, vol. 42, pp. 43–45, 1983.
- [13] J. S. Karp, L. E. Adam, R. Freifelder, et al. A high-resolution GSO-based brain PET camera. Proceedings of The IEEE 1999 Nuclear Science Symposium and Medical Imaging Conference, pp. 1077-81 vol.2, (Edited by J. A. Seibert), Seattle, WA, 1999.
- [14] A. Saoudi, C. M. Pepin, F. Dion, et al., "Investigation of depth-of-interaction by pulse shape discrimination in multicrystal detectors read out by avalanche photodiodes," *IEEE Trans. Nucl. Sci.*, vol. NS-46, pp. 462-467, 1999.
- [15] M. Schmand, L. Eriksson, M. Casey, et al., "Performance results of a new DOI detector block for a high resolution PET-LSO research tomograph HRRT," *IEEE Trans. Nucl. Sci.*, vol. NS-45, pp. 3000–3006, 1998.
- [16] J. S. Huber, W. W. Moses, M. S. Andreaco, et al., "A LSO scintillator array for a PET detector module with depth of interaction measurement," *IEEE Trans. Nucl. Sci.*, vol. NS-48, pp. (submitted for publication), 2001.
- [17] Y. P. Shao and S. R. Cherry, "A study of depth of interaction measurement using bent optical fibers," *IEEE Transactions On Nuclear Science*, vol. NS-46, pp. 618-623, 1999.
- [18] J. G. Rogers, C. Moisan, E. M. Hoskinson, et al., "A practical block detector for a depth-encoding PET camera," *IEEE Trans. Nucl. Sci.*, vol. NS-43, pp. 3240-3248, 1996.
- [19] R. S. Miyaoka, T. K. Lewellen, J. H. Yu, et al., "Design of a depth of interaction (DOI) PET detector module," *IEEE Trans. Nucl. Sci.*, vol. NS-45, pp. 1069-1073, 1998.
- [20] W. Worstell, O. Johnson, H. Kudrolli, et al., "First results with high-resolution PET detector modules using wavelength-shifting fibers," *IEEE Trans Nucl Sci*, vol. 45, pp. 2993-2999, 1998.
- [21] M. B. Williams, R. M. Sealock, S. Majewski, et al., "PET detector using waveshifting optical fibers and microchannel plate PMT with delay line readout," *IEEE Trans. Nucl. Sci.*, vol. 45, pp. 195–205, 1998.
- [22] A. P. Jeavons, R. A. Chandler, and C. A. R. Dettmar, "A 3D HIDAC-PET camera with sub-millimetre resolution for imaging small animals," *IEEE. Trans. Nucl. Sci.*, vol. NS-46, pp. 468-473, 1999.
- [23] V. Chepel, V. Solovov, J. van der Marel, et al., "The liquid xenon detector for PET: Recent results," *IEEE Trans. Nucl. Sci.*, vol. NS-46, pp. 1038-1044, 1999.
- [24] K. Murthy, M. Aznar, A. M. Bergman, et al., "Positron emission mammographic instrument: Initial results," *Radiology*, vol. 215, pp. 280-285, 2000.
- [25] N. K. Doshi, Y. P. Shao, R. W. Silverman, et al., "Design and evaluation of an LSO PET detector for breast cancer imaging," *Medical Physics*, vol. 27, pp. 1535-1543, 2000.
- [26] R. Freifelder and J. S. Karp, "Dedicated PET scanners for breast imaging," *Physics in Medicine and Biology*, vol. 42, pp. 2463-2480, 1997.
- [27] W. W. Moses, T. F. Budinger, R. H. Huesman, et al., "PET camera designs for imaging breast cancer and axillary node involvement," *J. Nucl. Med.*, vol. 36, pp. 69P, 1995.
- [28] A. F. Chatzioannou, S. R. Cherry, Y. P. Shao, et al., "Performance evaluation of microPET: A high-resolution lutetium oxyorthosilicate PET scanner for animal imaging," *Journal of Nuclear Medicine*, vol. 40, pp. 1164-1175, 1999.
- [29] A. Del Guerra, C. Damiani, G. Di Domenico, et al., "An integrated PET-SPECT small animal imager: preliminary results," *IEEE Trans Nucl Sci*, vol. NS-47, pp. 1537-1540, 2000.
- [30] A. P. Jeavons, "Small-animal PET cameras," *Journal of Nuclear Medicine*, vol. 41, pp. 1442-1443, 2000.
- [31] S. Siegel, J. J. Vaquero, L. Aloj, et al., "Initial results from a PET planar small animal imaging system," *IEEE Trans Nucl Sci*, vol. NS-46, pp. 571-575, 1999.
- [32] D. Lapointe, N. Brasseur, J. Cadorette, et al., "High-Resolution PET imaging for in vivo monitoring of tumor response after photodynamic therapy in mice," *Journal of Nuclear Medicine*, vol. 40, pp. 876-882, 1999.
- [33] T. Beyer, D. W. Townsend, T. Brun, et al., "A combined PET/CT scanner for clinical oncology," *Journal of Nuclear Medicine*, vol. 41, pp. 1369-1379, 2000.